



Arginyl-tRNA-protein transferase 1 (ATE1) promotes melanoma cell growth and migration

Ikrame Lazar, Bertrand Fabre, Yongmei Feng, Ali Khateb, Philippe Frit, Anna Kashina, Tongwu Zhang, Emily Avitan-Hersh, Hyungsoo Kim, Kevin Brown, et al.

► To cite this version:

Ikrame Lazar, Bertrand Fabre, Yongmei Feng, Ali Khateb, Philippe Frit, et al.. Arginyl-tRNA-protein transferase 1 (ATE1) promotes melanoma cell growth and migration. FEBS Letters, 2022, 596 (11), pp.1468-1480. 10.1002/1873-3468.14376 . hal-03745766

HAL Id: hal-03745766

<https://hal.science/hal-03745766>



Submitted on 23 Nov 2022

HAL is a multi-disciplinary open access archive for the deposit and dissemination of scientific research documents, whether they are published or not. The documents may come from teaching and research institutions in France or abroad, or from public or private research centers.

L'archive ouverte pluridisciplinaire **HAL**, est destinée au dépôt et à la diffusion de documents scientifiques de niveau recherche, publiés ou non, émanant des établissements d'enseignement et de recherche français ou étrangers, des laboratoires publics ou privés.

RESEARCH ARTICLE

Arginyl-tRNA-protein transferase 1 (ATE1) promotes melanoma cell growth and migration

Ikrame Lazar^{1,2,3} , Bertrand Fabre^{2,4}, Yongmei Feng¹, Ali Khateb^{1,2}, Philippe Frit⁵, Anna Kashina⁶, Tongwu Zhang⁷, Emily Avitan-Hersh², Hyungsoo Kim¹, Kevin Brown⁷, Ivan Topisirovic⁸  and Ze'ev A. Ronai¹

¹ Sanford Burnham Prebys Medical Discovery Institute, La Jolla, CA, USA

² Technion Integrated Cancer Center, Faculty of Medicine, Technion Institute of Technology, Haifa, Israel

³ MCD, Centre de Biologie Intégrative (CBI), CNRS, UT3, Université de Toulouse, France

⁴ Laboratoire de Recherche en Sciences Végétales, UMR5546, UT3, INP, CNRS, Université de Toulouse, Auzeville-Tolosane, France

⁵ Institut de Pharmacologie et de Biologie Structurale (IPBS), UMR 5089, CNRS, UT3, Université de Toulouse, France

⁶ Department of Biomedical Sciences, University of Pennsylvania, Philadelphia, PA, USA

⁷ Division of Cancer Epidemiology and Genetics, National Cancer Institute, Bethesda, MD, USA

⁸ Gerald Bronfman Department of Oncology, Departments of Experimental Medicine and Biochemistry, Lady Davis Institute, Sir Mortimer B. Davis Jewish General Hospital, McGill University, Montreal, QC, Canada

Correspondence

I. Lazar, Sanford Burnham Prebys Medical Discovery Institute, La Jolla, CA 92037, USA

Tel: +33(0)561558894

E-mail: ikrame.lazar@univ-tlse3.fr

(Received 8 August 2021, revised 21 April 2022, accepted 25 April 2022, available online 20 May 2022)

doi:10.1002/1873-3468.14376

Edited by Lukas Alfons Huber

Arginyl-tRNA-protein transferase 1 (ATE1) catalyses N-terminal protein arginylation, a post-translational modification implicated in cell migration, invasion and the cellular stress response. Herein, we report that *ATE1* is overexpressed in NRAS-mutant melanomas, while it is downregulated in BRAF-mutant melanomas. *ATE1* expression was higher in metastatic tumours, compared with primary tumours. Consistent with these findings, *ATE1* depletion reduced melanoma cell viability, migration and colony formation. Reduced *ATE1* expression also affected cell responses to mTOR and MEK inhibitors and to serum deprivation. Among putative *ATE1* substrates is the tumour suppressor AXIN1, pointing to the possibility that *ATE1* may fine-tune AXIN1 function in melanoma. Our findings highlight an unexpected role for *ATE1* in melanoma cell aggressiveness and suggest that *ATE1* constitutes a potential new therapeutic target.

Keywords: ATE1; AXIN1; cancer; cell migration; cell viability; melanoma

Arginyl-tRNA-protein transferase 1 (ATE1) is the only known mediator of N-terminal arginylation of proteins in mammals [1]. This post-translational modification involves the addition of an arginine (Arg) moiety to exposed N-terminal aspartate (Asp), glutamate or oxidized cysteine (Cys) residues and requires a prior step of methionine (Met) removal or protein cleavage [1]. N-terminal arginylation acts as a degradation signal for proteins via the Arg/N-degron pathway, which

involves recognition of proteins with certain N-terminal amino acids by specific binding proteins known as N-recognins, followed by ubiquitination and proteasomal degradation of the protein [1].

In addition to the role in regulating protein stability by the ubiquitin–proteasome system, the consequences of N-terminal arginylation have recently been broadened to include additional aspects of protein regulation. For example, N-terminal arginylation of the

Abbreviations

ATCC, American Type Culture Collection; ATE1, arginyl-tRNA-protein transferase 1; CCLE, cancer cell line encyclopedia; ERK, extracellular signal-regulated kinase; KD, knockdown; KO, knockout; MAPK, mitogen-activated protein kinase; MEF, mouse embryonic fibroblasts; MEK, mitogen-activated protein kinase kinase; mTOR, mammalian target of rapamycin; TCGA, The Cancer Genome Atlas.

chaperone GRP78/BiP induces its translocation from the endoplasmic reticulum to the cytosol, where GRP78/BiP interacts with the autophagy adaptor protein SQSTM1/p62 and is targeted for degradation in autophagosomes [2]. Moreover, N-terminal arginylation of phosphoribosyl pyrophosphate synthase 2 (PRPS2) promotes its enzymatic activity without affecting its half-life [3]. ATE1 knockout (KO) in mice leads to embryonic lethality due to cardiovascular defects [4]. Platelet-specific ATE1 KO impairs myosin function and regulation of clotting [5], while neural-specific ATE1 KO impairs neurite outgrowth [6]. Conditional ATE1 deletion in murine neural crest cells impairs their migration and leads to abnormal growth, respiration, mental defects and perinatal death [7]. ATE1 has also been implicated in the regulation of cell survival. For example, ATE1 attenuates cell death in T-RExTM-293 cells, by promoting the degradation of pro-apoptotic fragments formed by caspases [8]. Along these lines, ATE1 KO sensitizes mouse embryonic fibroblasts (MEFs) to apoptosis [8]. ATE1 has been also implicated in the cellular stress response. ATE1 KO MEFs are more sensitive to heat stress, possibly *via* N-terminal arginylation of human antigen R, which controls the mRNA stability of heat-shock protein 70.3 [9]. Despite the enhanced sensitivity to heat stress, ATE1 KO MEFs are more resistant than wild-type MEFs to oxidative stress, suggesting that a distinct set of ATE1 substrates affect cellular stress response pathways [10].

Consistent with the diverse cellular functions of ATE1, dysregulation of its activity has been linked to a number of pathological disorders, including neurodegenerative diseases [11] and cancer [12]. Importantly, ATE1 KO in MEFs is sufficient to induce tumour formation after injection into nude mice suggesting that ATE1 may play a role as a tumour suppressor [12]. Consistent with this, *ATE1* mRNA expression levels are inversely correlated with the progression of human kidney, colon and prostate tumours [12,13]. In contrast, several reports suggest that ATE1 may have oncogenic properties. ATE1 is required for cell migration of motile cells, through a mechanism involving β -actin arginylation. Consequently, in ATE1 KO MEFs, inhibition of this event prevents the formation of lamellipodia and blocks locomotion [14,15]. In addition, Arg deprivation inhibits cell adhesion and invasiveness of glioblastoma cells, a phenotype that was linked to inhibition of β -actin arginylation [16]. The ability of ATE1 to exert oncogenic or tumour suppressor functions may thus be specific of cell or tissue type [12,13,17].

Melanoma is the most aggressive form of skin cancer, primarily due to its strong propensity to

metastasize [18]. Both genetic and epigenetic changes in melanocytes have been implicated in re-activation of neural crest lineage cells [19,20]. Given that ATE1 plays important roles in neural crest cells during embryonic development, including migration [7], we set to assess whether ATE1 may contribute to melanomagenesis and/or key phenotypes associated with metastatic capacity.

Results

ATE1 expression is deregulated in melanoma

We first investigated if *ATE1* expression correlates with melanoma patient prognosis using The Cancer Genome Atlas (TCGA) data sets. This analysis revealed no association between *ATE1* mRNA level and melanoma patient survival ($P = 0.872$) (Fig. S1A). However, we observed a significant enrichment in metastatic tumours in the *ATE1* expression high group (fisher's exact P -value = 0.00089, Odd ratio = 4.2). In addition, we observed higher age at diagnosis and enrichment in male patients in the *ATE1* expression high group although these differences did not reach significant P -values (Fig. S1B, Table S1). Interestingly, when adjusting TCGA data using the age, the type of tumour and the gender of the patients, we observed that *ATE1* high expression is associated with decreased survival ($P = 0.0002499$) (Fig. S1A, Table S1). We then examined *ATE1* expression in melanoma tumours by analysis of a transcriptome data set of both transcriptome and genome data set of 415 melanoma patients from TCGA. We selected and compared the genomic features between tumours with highest (20%, $N = 83$) and lowest (20%, $N = 83$) *ATE1* expression (Fig. 1A). Approximately 50% and 20% of human melanomas harbour mutations in BRAF and NRAS signalling proteins, respectively [21]. Further assessment of the TCGA data set indicated that the majority (70%) of *ATE1*-low tumours harboured mutant BRAF, while mutant NRAS was the most common mutation (46%) in melanomas with high *ATE1* expression (Fig. 1B). These findings suggest that dysregulated *ATE1* expression may be linked to the type of driver mutation and thus could potentially play a context-specific role in melanoma progression.

We compared ATE1 expression in BRAF-mutant A375 and 1205Lu and NRAS-mutant WM1366 melanoma cell lines at the mRNA and protein levels. Although no differences in *ATE1* expression were observed at the mRNA level between the 1205Lu (BRAF) and WM1366 (NRAS) cell lines (A375 being higher than both other cell lines), ATE1 protein

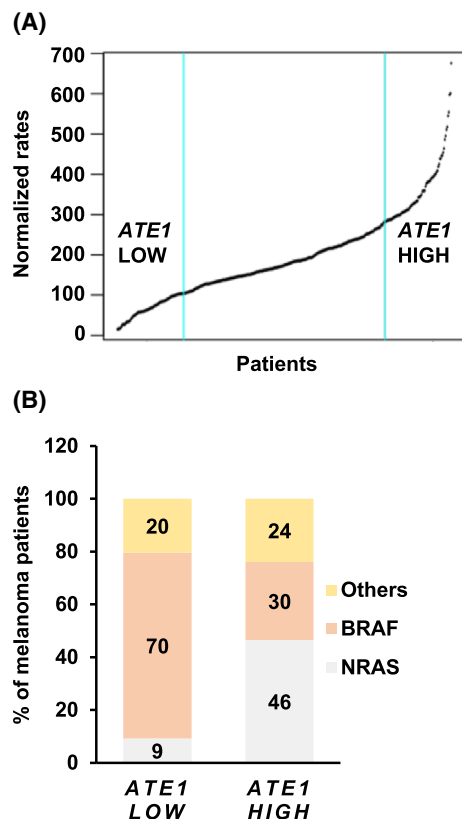


Fig. 1. *ATE1* expression is deregulated in melanoma. (A) *ATE1* expression level in a TCGA melanoma patient cohort ($n = 415$). The cut-off values for patients with highest ($n = 83$) and lowest ($n = 83$) *ATE1* expression are indicated by blue vertical lines. (B) Percentage of melanoma patients within the *ATE1*-high and -low groups harbouring BRAF, NRAS, and other mutations.

expression was higher in WM1366 (NRAS) compared with 1205Lu (BRAF) suggesting that *ATE1* expression might be regulated post-transcriptionally in these cell lines (Fig. S2A).

In addition, we monitored *ATE1* expression in a larger number of melanoma cell lines using the Cancer Cell Line Encyclopedia (CCLE) data sets [22]. *ATE1* level tends to be higher in NRAS-mutant group although the results were not significantly different due to the low number of NRAS-mutant cell lines (Fig. S2B). Overall, these data suggest that the difference in *ATE1* expression observed in patients might not be completely recapitulated in melanoma cell lines although the trend is similar.

ATE1 is associated with melanoma cell migration and melanoma metastasis

To determine the role of *ATE1* in key malignant phenotypes of melanoma cells, we examined the effects of

ATE1 knockdown (KD) with two different short hairpin (sh) RNAs (Fig. S3A) on the migration of human and mouse BRAF- and NRAS-mutant melanoma cell lines. As expected, in both BRAF-mutant (1205Lu) and NRAS-mutant (WM1366) human melanoma cell lines, *ATE1* KD cells exhibited decreased focal adhesion structures compared with cells transduced with control empty vector (Fig. 2A). Consistent with deregulation of the cytoskeleton, *ATE1* KD significantly reduced cell migration in both cell lines, an observation that was particularly noted in 1205Lu cells (Fig. 2B). A similar reduction in migration upon *ATE1* KD was observed in the murine NRAS-mutant melanoma cell line SW1 (Fig. S3A and Fig. S3B). Because migratory potential is a key feature of the metastatic process, we compared *ATE1* expression in TCGA data sets of metastatic ($n = 368$) or primary ($n = 103$) melanoma samples. Interestingly, *ATE1* was expressed at a significantly higher levels in metastatic samples (Fig. 2C). Thus, *ATE1* expression may contribute to migration and the metastatic phenotype of melanoma.

ATE1 knockdown inhibits melanoma cell viability and colony-forming ability

We next assessed the effects of *ATE1* KD on viability of melanoma cells (Fig. S4A) using CellTiter Glo kit which is based on ATP level measurement. *ATE1* KD effectively inhibited viability of NRAS-mutant cell lines (WM1366 and SW1, Fig. 3A) and BRAF-mutant cell line 1205Lu but not A375 BRAF-mutant cell line (Fig. 3A). Given that *ATE1* has been involved in mitochondrial functions [23], we confirmed its effect on WM1366 cell line viability by live-imaging and using a crystal-violet-based assay which are ATP-independent method (Fig. S4B,C). Notably, the effect of *ATE1* depletion was less pronounced in the BRAF than in NRAS-mutant cell lines. Concomitant with an inhibition of cell viability, *ATE1* KD promoted cell death in WM1366 cells (Fig. S4C). In contrast, colony formation in 3-dimensional (3D) cultures was equally impaired upon *ATE1* KD of BRAF- and NRAS-mutant cell lines (Fig. 3B and Fig. S4D, respectively). Moreover, viability suppression by *ATE1* KD appears specific of melanoma cells, because loss of *ATE1* in MEFs conferred a survival advantage (Fig. S4E). These observations point to distinct cellular functions for *ATE1* in behaviours associated with specific driver mutations, such as the possible greater dependence of NRAS-mutant than BRAF-mutant melanoma cell lines on *ATE1* to maintain cell viability. However, cancer cell lines bearing numerous mutations, the

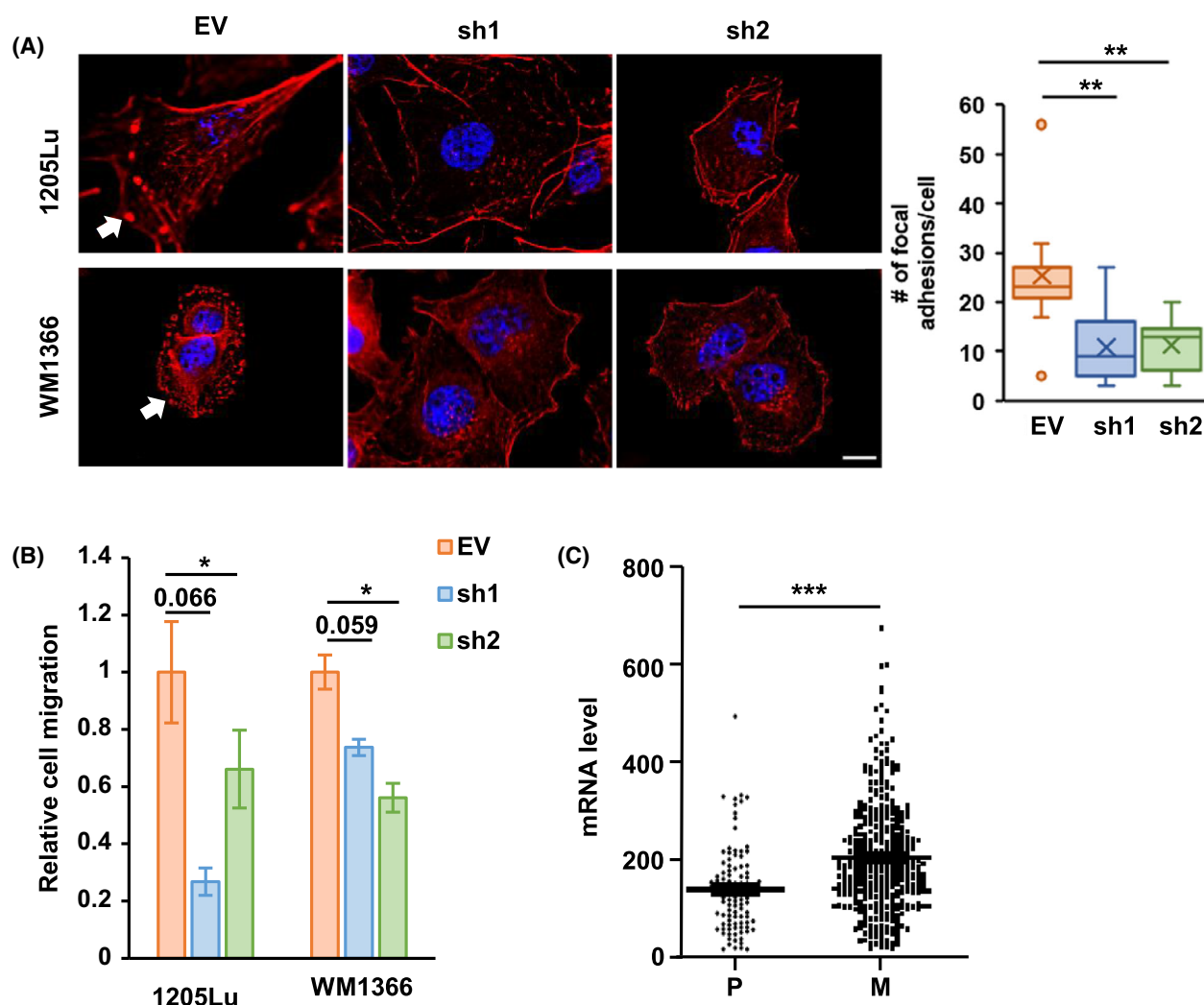


Fig. 2. ATE1 is required for melanoma cell migration and is overexpressed in metastatic melanomas. (A) Left: Fluorescence staining of actin (red) in the indicated melanoma cell lines transduced with empty vector (EV) or two ATE1-targeting shRNAs. Nuclei are stained with DAPI (blue). Scale bar: 10 μ m. White arrows indicate focal adhesions that were decreased in ATE1 KD cells. Right: quantification of focal adhesions at the cell periphery in WM1366 cells. The boxplots represent the distribution of the number of focal adhesions per cell for each condition. (B) Migration assay of the indicated melanoma cells transduced as described in (A). $N = 3$. (C) ATE1 mRNA levels in TCGA datasets of primary (P, $n = 103$) and metastatic (M, $n = 368$) melanomas. Mean \pm SEM. * $P < 0.05$, *** $P < 0.001$ by Student's t -test.

dependency of NRAS-mutant cancer cells should be further investigated in larger number of cell lines or in isogenic models carrying either BRAF or NRAS mutations.

ATE1 plays a role in the response of melanoma cells to stress

Having established that ATE1 influences the viability behaviours of melanoma cells, we next determined whether ATE1 plays a role in the adaptation to stress induced by serum and/or glutamine (Gln) deprivation (Fig. 4A). Notably, we observed an increase in the

molecular weight of ATE1 in A375 cells incubated in the absence of serum or both serum and Gln, but not in the absence of Gln alone (Fig. 4B). ATE1 molecular shift under serum deprivation was also observed in WM1366 cell line (Fig. S5A), suggesting that ATE1 itself may undergo an unknown post-translational modification under stress induced by serum, but not Gln, restriction. Among the lines tested, 1205Lu cells retained the ability to grow in the absence of serum, albeit at a slower rate (Fig. S5B). ATE1 silencing rendered 1205Lu cells even more sensitive to serum starvation (Fig. 4C). These data indicate that ATE1 contributes to the nutrient deprivation stress response in melanoma cells.

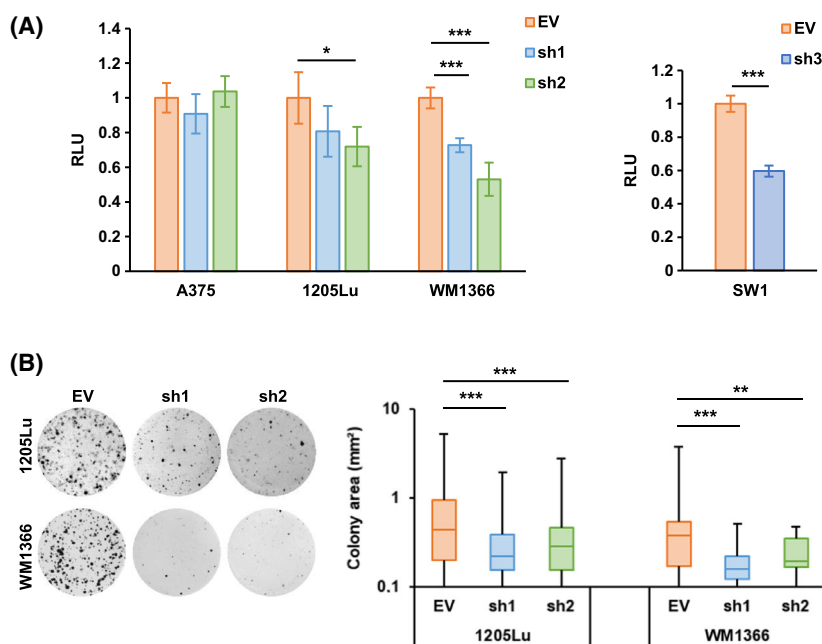


Fig. 3. ATE1 knockdown inhibits melanoma cell viability and colony-forming ability. (A) Cell viability assay using CellTiter Glo Kit 72 h after seeding the indicated melanoma cell lines transduced with empty vector (EV) or ATE1-targeting shRNA. Mean \pm SEM. $N \geq 3$. RLU: relative luminescence units. (B) Plate images (left) and quantification (right) of colony formation by the indicated melanoma cell lines transduced as described in (A). Boxplots show the median, and the first and third quartiles. * $P < 0.05$, ** $P < 0.01$, *** $P < 0.001$ by Student's *t*-test.

To explore this finding further, we assessed the activation status of two key regulators of the cellular response to nutrient deprivation; the MAPK and mTOR signalling pathways [24,25]. As a readout of pathway activation, we performed western blot analysis of the activation (phosphorylation) status of the enzymes S6K and ERK, which lie downstream in the mTOR and MAPK signalling pathways, respectively.

In the presence of serum in the culture media, ATE1 KD cells exhibited a lower level of phosphorylated S6K compared with control cells. This level was comparable with the one observed under serum restriction in control cells (Fig. 5A and Fig. S6A). Consistent with this result, ATE1 KD in WM1366, SW1 and 1205Lu cells sensitized cells to the mTOR inhibitor, torin 1 (Fig. 5B and Fig. S6B). However, ATE1 KD led to an opposite effect on MAPK pathway with higher level of phosphorylated ERK in ATE1 KD WM1366 and SW1 cells compared with control cells (Fig. 5A and Fig. S6A) and a lower sensitivity to the MEK inhibitor PD0325901 in WM1366, 1205Lu and SW1 cells (Fig. 5C and Fig. S6C) or to the BRAF inhibitor PLX4032 in 1205Lu cells (Fig. S6D).

AXIN1 level is affected by ATE1

The observation that ATE1 has differing effects on the mTOR and MAPK signalling led us to examine the possible mediators (ATE1 substrates) that may mediate these changes. To this end, we performed an

in vitro arginylation assay [26] that detects ATE1-mediated N-terminal arginylation of an array of N-terminal peptides containing putative arginylation sites. In this case, the N-terminal peptides were derived from 79 proteins associated with the regulation of the mTOR or MAPK pathways. As controls, we included a set of peptides without Asp or Glu N-terminal amino acids (Table S2) and of the same peptides with a N-terminal acetylation, which prevents arginylation [1]. Among the potential ATE1 substrates identified, the strongest specific signal was obtained with the N-terminal peptide of AXIN1, that in addition to its role in Wnt/ β -catenin signalling [27] has also been reported to suppress mTOR pathway [28] (Fig. 6A,B). Consistent with the possibility that AXIN1 is an ATE1 substrate, we found that AXIN1 protein expression was upregulated by ATE1 knockdown in WM1366 cells (Fig. 6C) and 1205Lu cells (Fig. S7A) and, conversely, AXIN1 was downregulated by ATE1 overexpression in WM1366 cells (Fig. 6D). Importantly, AXIN1 mRNA levels were unaffected by ATE1 knockdown, confirming that alterations in AXIN1 abundance was mediated at the protein level (Fig. 6E). However, AXIN1 stability was not affected following ATE1 knock down in WM1366 suggesting that ATE1 does not affect AXIN1 degradation and rather points toward an alternative regulation of AXIN1 protein level (e.g. regulation of AXIN1 synthesis rate) (Fig. S7B). Altogether, these data identify AXIN1 as a potential ATE1 substrate in melanoma cells and may link ATE1 to mTOR signalling.

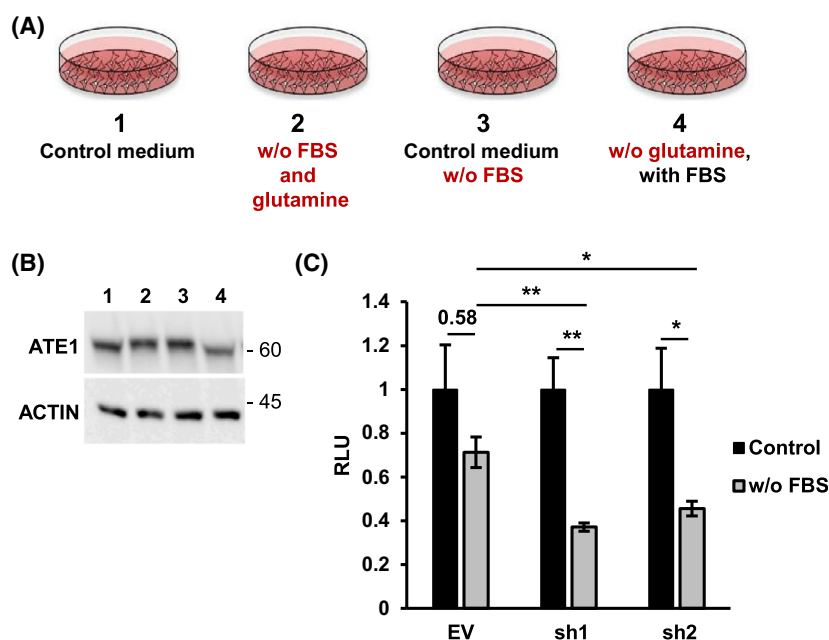


Fig. 4. ATE1 knockdown sensitizes melanoma cells to serum starvation. (A) Schematic representation of the four culture conditions tested. (B) Western blot analysis of ATE1 and β -actin (loading control) in A375 cells incubated for 12 h under the conditions shown in (A). (C) Cell viability assay using CellTiter Glo Kit of Lu1205 cells transduced with empty vector (EV) or ATE1-targeting shRNAs and grown in the presence or absence of FBS. Mean \pm SEM. * P < 0.05, ** P < 0.01, *** P < 0.001 by Student's t -test. RLU, relative luminescence units.

Discussion

The present study identifies ATE1 as an unexpected player in melanomagenesis. High and low *ATE1* expression levels in clinical specimens correlated with the presence of driver mutations in NRAS and BRAF, respectively. In addition, stratifying metastatic melanomas depending on their genotype revealed higher *ATE1* level in the NRAS mutant group (Fig. S8) suggesting that NRAS signalling may strongly promote *ATE1* expression, possibly via intermediates or, pathways that are relatively weakly induced by mutant BRAF [29–31]. A selective increase in *ATE1* expression in NRAS-mutant tumours may provide advantages by driving processes that are not activated in BRAF-mutant tumours. Thus, targeting ATE1 may offer a unique therapeutic modality for NRAS-mutant tumours, which remains an unmet clinical need.

Consistent with this hypothesis, we found that the survival of NRAS-mutant melanoma cells was more dependent on ATE1 compared with BRAF-mutant cells. This observation implicates ATE1 in attenuating cell death/autophagy signalling, which is commonly seen in NRAS-mutant melanomas [32]. In contrast to survival, ATE1 expression was equally important in supporting the migration of BRAF- and NRAS-mutant melanomas, indicating that signalling pathways common to both driver mutations (e.g. ERK) may underlie the contribution of ATE1 to the migration phenotype. Thus, while the involvement of ATE1 in some fundamental processes, such as migration and

metastasis, may occur via a mechanism activated by both NRAS and BRAF mutations, ATE1 contribution to other phenotypes, such as survival, may occur exclusively in NRAS-mutant tumours. Given that NRAS and BRAF mutations are present in about 75% of melanomas, ATE1 is expected to exert numerous promoting functions in this tumour type.

In contrast to our observations in melanoma, *ATE1* expression was found to correlate inversely with tumour progression in human kidney, colon and prostate cancer [12,13], indicating a tumour suppressor function. The opposing functions of ATE1 in melanoma cells compared with these cancers could be due to several factors, including the presence of different driver mutations in oncogenes and tumour suppressor genes, as well as epigenetic changes that may define not only ATE1 expression and activity levels but also its specific substrates in different cell types. Such differences would be consistent with the distinct landscape of mutations implicated in kidney, prostate and colon tumours [33]. Among factors that may underlie the tumour-promoting role of ATE1 compared with its tumour suppressor role in other tumour types may be related to high prevalence of NRAS mutations in melanoma [34,35] but rare in prostate, kidney and colon tumours. Consistent with this hypothesis, pancreatic cancer samples, 95% of which harbour mutant KRAS, exhibit high level of *ATE1* expression compared with control tissues [36] (Fig. S9). In this regard, understanding the role of ATE1 in pancreatic cancer

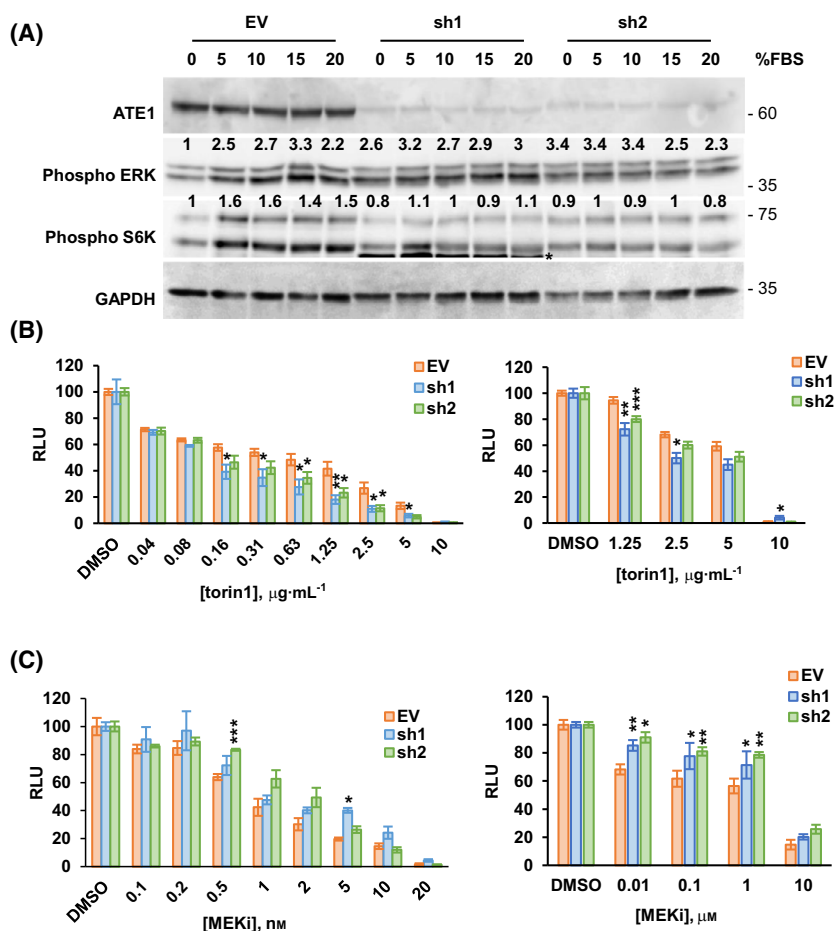


Fig. 5. ATE1 knockdown differentially sensitizes melanoma cells to mTOR and MAPK pathway inhibitors. (A) Western blot analysis of ERK and S6K phosphorylation in WM1366 cells transduced with empty vector (EV) or ATE1-targeting shRNAs and grown in the absence or presence of serum (FBS) for 12 h. Numbers below each lane indicate band intensities normalized to the corresponding GAPDH signals. * in phospho-S6K lanes indicates a nonspecific band. (B, C) Cell viability assays using CellTiter Glo Kit of WM1366 (left) or 1205Lu (right) cells transduced as described in (A) and grown in the presence of the indicated concentrations of (B) the mTOR inhibitor Torin1 or (C) the MEK inhibitor PD0325901 for 48h and 72 h respectively. RLU, relative luminescence units. Mean \pm SEM. * $P < 0.05$, ** $P < 0.01$, *** $P < 0.001$ by Student's *t*-test.

will undoubtedly provide novel insights into the mechanisms underlying pancreatic development and/or progression. Clearly, large-scale proteomic-based comparisons of different tumour types could be helpful in identifying differences in the expression, activity, localization and substrates of ATE1. Of note, the decreased viability observed upon ATE1 knockdown is consistent with the phenotype observed in the hepatoma Hepa1-6 (hepatoma) and hepatocytes AML-12 cell lines upon modulation of expression of different Arg/N-degron pathway components (e.g. UBR1, -2, -4 and -5; [37]).

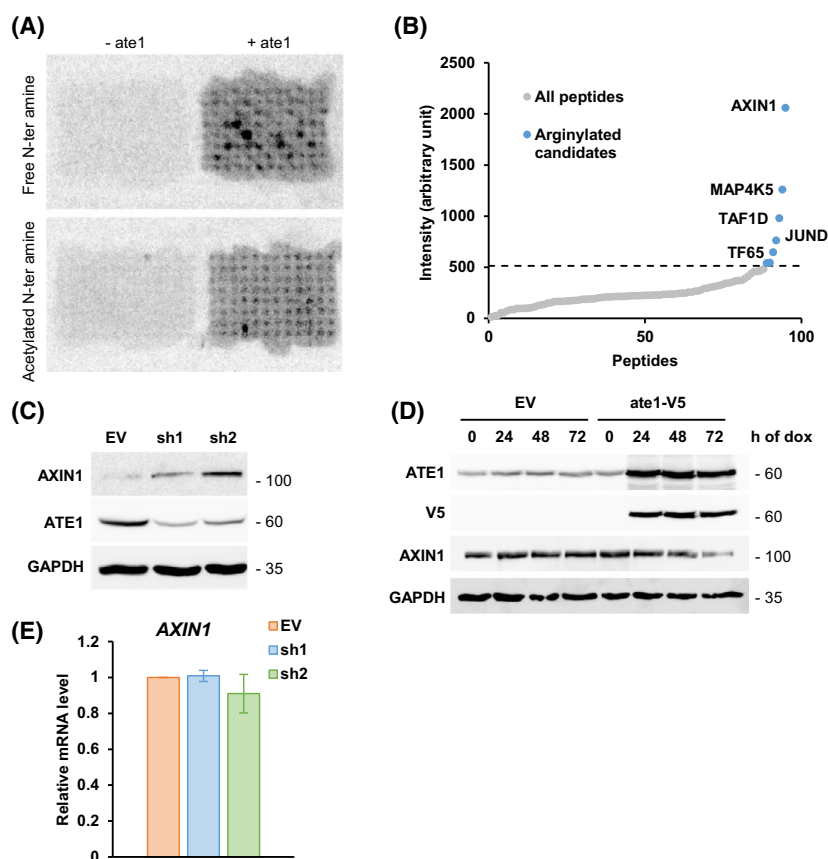
Our observation that ATE1 knockdown disrupted actin organization and inhibited migration of melanoma cells is consistent with independent reports showing that inhibition of protein arginylation impairs β -actin function and organization with consequent effects on the migration of MEF cells [14,15]. ATE1 activity may be particularly important for cell migration in tumours with a strong propensity to metastasize, such as melanomas. Evidence that ATE1 function may depend on the tumour cell lineage of origin comes

from reports that ATE1 is essential for the migration of neural crest cells [7], which originate from the ectoderm and also give rise to melanocytes [38]. Moreover, neural crest lineage cells are responsible for some of the more aggressive forms of prostate cancer, such as the neuroendocrine form [39], which suggests that further studies should investigate the possible importance of ATE1 in neuroendocrine prostate tumours such as the hormone refractory forms.

We show that serum starvation of melanoma cells caused an increase in the molecular weight of ATE1, raising the possibility that ATE1 is subject to post-translational modification. Such alterations can affect a range of protein properties, such as enzymatic activity, subcellular localization and substrate selectivity, highlighting the need for further work to identify the precise modifications of ATE1. We speculate that the molecular weight change identified here is likely to be linked to an increase in ATE1 activity, as ATE1 knockdown enhanced the effect of serum starvation on melanoma cell viability. Our initial investigations of possible factors involved in the ATE1 modification

Fig. 6. AXIN1 level is affected by ATE1.

(A) *In vitro* [^{14}C]-arginylation assay using CelluSpot arrays of MAPK and mTOR pathway N-terminal peptides. (B) [^{14}C]-arginine intensities of peptides ranked from lowest to highest intensity. The threshold for designation of candidate proteins (515 arbitrary units) was determined as described in Experimental Procedures. (C) Western blot analysis of AXIN1 and ATE1 in WM1366 cells transduced with empty vector (EV) or ATE1-targeting shRNAs. (D) Western blot analysis of the indicated proteins in WM1366 cells transduced with EV or an ATE1 overexpression vector (V5) following induction with 500 ng·mL $^{-1}$ doxycycline (dox) for 24, 48, or 72 h. (E) RT-qPCR analysis of *AXIN1* mRNA levels in WM1366 cells transduced as described in (C). Mean \pm SEM, $N = 2$.



excluded both Gln and glucose, because their deprivation did not induce the shift in ATE1 molecular weight. Nevertheless, our observation that ATE1 knockdown modulates two important pathways in the cellular response to stress, mTOR and MAPK, implicates other nutrients, such as amino acids and growth factors, in the post-translational modification of ATE1.

Identifying how ATE1 senses changes in nutrient availability and regulates the mTOR and MAPK signalling pathways remain important questions for understanding the role of ATE1 in key cellular regulatory networks. The results of this study provide the first clues to the identity of potential ATE1 substrates that may control these signalling pathways. We employed an *in vitro* peptide array assay to probe ATE1-mediated arginylation of N-terminal peptides from proteins associated with the MAPK and mTOR signalling pathways, and identified AXIN1, MAP4K5 and JUND as putative substrates. We focused on AXIN1 for several reasons: it was the most strongly arginylated peptide in the array, it plays an important role in promoting β -catenin/CTNNB1 degradation [40], it has been suggested to have a tumour

suppressor role in several tumour types, including hepatocellular carcinoma [41,42], and it has been shown to control transcription of the tumour suppressor TP53/p53 and to regulate the cell death program in HeLa cells [43]. Notably, AXIN1 contains a tertiary N-degron, meaning that Met removal and deamidation by NTAN1 are required prior to the arginylation step, and that ATE1 likely affects AXIN1 availability. ATE1 is known to form a complex with NTAN1 and NTAQ1 amidases and UBR1 ubiquitin ligase, suggesting that the deamidation step is coupled to arginylation [44]. Although removal of Met before Asp, Glu, Asn or Gln may be considered an unlikely event because of spatial constraints [45], it has been shown to occur during N-terminal Met acetylation-dependent cleavage of β -actin [46]. However, we observe that although ATE1 depletion increased AXIN1 protein level, this effect does not seem to point toward the regulation of AXIN1 protein degradation (Fig. S7B). Other mechanisms of regulation of protein expression might be involved, such as regulation of protein synthesis rate. It was indeed previously shown that ATE1 can associate with the translation machinery [47] pointing towards a function of ATE1 and arginylation

in protein synthesis. Nevertheless, further investigation would be needed to precise how ATE1 regulates protein synthesis and AXIN1 protein level. Whether these changes in AXIN1 level occur in an ATE1-dependent manner in melanoma cells will be an important question for future studies.

In conclusion, we have identified a role for ATE1 in the viability, migration and stress response of melanoma cells, suggesting that ATE1 has an unexpected tumour-promoting function. This is supported by observations of high *ATE1* expression in a subset of human melanomas, particularly those harbouring mutant *NRAS*. Although further work will be needed to pinpoint the precise contribution of ATE1 to the development and progression of melanoma, our results suggest that the catalytic activity of ATE1 could be a novel therapeutic target for *NRAS*-mutant tumours.

Experimental procedures

Cell culture

HEK293T, A375 and 1205Lu were obtained from the American Type Culture Collection (ATCC); WM1366 cells were from the Wistar Institute; and the murine melanoma cell line SW1, derived from a K-1735p lung metastasis [48] was a gift from Dr Margaret Kripke. All cell lines were grown in DMEM supplemented with 10% fetal bovine serum (FBS), 125 mg·mL⁻¹ streptomycin, and 125 UI·mL⁻¹ penicillin (GIBCO-Thermo Fisher Scientific, Waltham, MA, USA) and were maintained at 37 °C in a humidified atmosphere with 5% CO₂. Cells were cultured for up to 6 weeks and were examined regularly for mycoplasma contamination using a luminescence-based kit (Lonza, Basel, Switzerland). Melanoma cell lines were authenticated by short tandem repeat analysis at the Sanford Burnham Prebys Medical Discovery Institute Genomics core facility.

Reagents

PD0325901, Torin1 and PLX4032 were obtained from Selleckchem, cycloheximide, doxycycline and puromycin were from Merck (Rahway, NJ, USA), and phalloidin-conjugated rhodamine was from Molecular Probes (Waltham, MA, USA).

Plasmids

pCB410, a bacterial expression vector encoding the murine ATE1 variant 1A7B, was a kind gift from Dr. Alexander Varshavsky. Murine ATE1 variant 1A7B in pBabe vector was a kind gift from Dr. Anna Kashina

and was subcloned into pLVX TetOne-puro plasmid (Clontech) using NEBuilder® HiFi DNA Assembly kit (New England Biolabs) as previously described [49]. Primer sequences used to generate these constructs are available upon request. Lentiviral pLKO.1 vectors expressing human ATE1-specific shRNAs were obtained from the La Jolla Institute for Immunology RNAi Center (La Jolla, CA, USA). Target sequences were as follows: ATE1 sh#1, CGGGTGACTTTGCA TTGATAA; ATE1 sh#2, GATGACATCAAAGAGAGTTTA; and Ate1 sh#3, ATGAGAATCTTGTGGTTAATA.

Cell transduction

Lentiviral transduction was performed as previously described [49]. Briefly, lentiviral particles were prepared by transfection of HEK293T cells with ATE1 shRNA or ATE1 expression vector and the second-generation packaging plasmids ΔR8.2 and Vsv-G (Addgene, Watertown, MA, USA). Virus-containing supernatants were collected, mixed with polybrene (Merck) to pre-seeded melanoma cells. After 24 h, cells were transferred to 10-cm culture dishes for selection with puromycin (Merck).

ATE1 expression analysis in melanoma patient samples

To investigate the genomic alterations associated with *ATE1* expression, we explored the gene expression, driver gene mutation and survival data from the TCGA SKCM data set through cBioPortal (<https://www.cbioportal.org>, Skin Cutaneous Melanoma, TCGA PanCancer Atlas, *n* = 415). Melanoma tumours were sorted according to *ATE1* expression (RNA Seq v2 RSEM) and top 20% tumour samples (*n* = 166) were selected for downstream analysis including 83 samples with highest *ATE1* expression and 83 samples with lowest *ATE1* expression). The mutation status of major melanoma driver genes (including *BRAF*, *NRAS*, *NFI*, *PTEN*, *TP53*, *KRAS* and *NRAS*) was compared between *ATE1* high and low groups.

Fluorescence microscopy

Cells were fixed with 4% paraformaldehyde for 20 min at room temperature, permeabilized with 0.2% Triton X-100 for 5 min and then blocked with phosphate-buffered saline (PBS) containing 0.2% Triton X-100 and 10% FBS for 30 min. Cells were incubated for 1 h with 6.6 μM rhodamine-conjugated phalloidin diluted in PBS containing 1% bovine serum albumin

(Merck). Cells were washed, mounted using Fluoroshield Mounting Medium containing 4',6-diamidino-2-phenylindole (DAPI) (Merck) and visualized using a fluorescence microscope DMi8 (Leica, Wetzlar, Germany) with a 100X oil immersion objective. All images were processed with the same parameters using the 3D deconvolution tool from LASX software (Leica).

Migration assay

Migration assays were performed as previously described [49]. Briefly, cells were collected with Accutase (Merck), resuspended in medium containing 1% FBS, and placed in the upper compartments of Transwell chambers (Corning, Corning, NY, USA). Medium containing 10% FBS was placed in the lower compartments and the plates were incubated at 37 °C for 24 h. The cells were fixed by addition of 4% paraformaldehyde for 10 min and stained with 0.4% crystal violet in 70% ethanol for 15 min. To quantify migrated cells, crystal violet was solubilized by addition of 10% acetic acid, and the optical density (OD) at 595 nm was measured using an Infinite 2000 Pro reader (Tecan, Männedorf, Switzerland).

Western blot analysis

Western blotting was performed as previously described [49]. Primary antibodies were as follows: rat anti-ATE1 (Merck Millipore; clone 6F11), mouse anti-GAPDH (Abcam, Cambridge, UK; ab8245), mouse anti-actin (08691001, MP Biomedicals, Irvine, CA, USA), mouse anti-tubulin (T9026, Merck), rabbit anti-ERK (#4695), rabbit anti-phosphorylated ERK (#4370), rabbit anti-phosphorylated S6K (Thr421/Ser424, #9204), rabbit anti-V5 (#13202) and rabbit anti-AXIN1 (#2087) (all from Cell Signaling Technology). HRP-conjugated secondary antibodies were purchased from Jackson ImmunoResearch (Ely, UK) and proteins were visualized by chemiluminescence (Image-Quant LAS400, GE Healthcare, Chicago, IL, USA).

RT-qPCR analysis

RNA was extracted from cells using the phenol/chloroform method and concentrations were measured using a NanoDrop spectrophotometer (ThermoFisher, Waltham, MA, USA). Reverse transcription was performed with aliquots of 1 µg total RNA using a qScript cDNA Synthesis Kit (Quanta, Houston, TX, USA). Quantitative PCR was performed with SYBR Green I dye master mix (Roche, Basel, Switzerland) and a CFX connect Real-Time PCR System (Bio-

Rad). *AXIN1* primers were as follows: forward ACAGGATCCGTAAGCAGCAC and reverse GGTA CGTGCGGGGAATGT. *H3A* primers were used as internal controls: forward AAGCAGACTGCCCCG CAAAT and reverse GGCCTGTAACGATGAGG TTTC. Primer efficiency was measured in preliminary experiments, and amplification specificity was confirmed by dissociation curve analysis.

Viability assay

Viability assays were performed using CellTiter Glo kits (Promega) as previously described [49]. Luminescence intensity was measured using an Infinite 2000 Pro reader (Tecan).

Colony formation assay

Cells were seeded in 6-well plates at 10^3 per well and incubated in a humidified atmosphere at 37 °C for 7–10 days. Colonies were fixed and stained using a ready-to-use solution of crystal violet (Merck). Plates were imaged with a scanner (Epson, Nagano, Japan) and colonies were analysed with IMAGEJ software (Bethesda, MD, USA).

Production of recombinant ATE1 and *in vitro* arginylation

Production of recombinant ATE1 and analysis of arginylation *in vitro* using CelluSpot[®] peptide arrays were performed as previously described [26]. In brief, transformed BL21(DE3) pLysS competent bacteria (Promega) were grown to an OD of 0.6 and ATE1 expression was induced by the addition of isopropyl β-D-1-thiogalactopyranoside at 0.25 mM for 6 h at room temperature. Cells were then centrifuged at 5000 *g* for 10 min at 4 °C and the pellets were lysed in 15 mL of PBS containing 30% glycerol, 0.3 M NaCl, 12 mM imidazole, 20 mM β-mercaptoethanol and 1 mg·mL⁻¹ lysozyme. The lysate was centrifuged at 15 000 *g* for 30 min at 4 °C, and the supernatant was removed and incubated with 5 mL of pre-washed nickel-agarose beads (GoldBio, St. Louis, MO, USA) for 4 h. The beads were washed five times with buffer A (20 mM Tris-HCl pH 7.5, 150 mM NaCl, 20 mM imidazole, 5 mM β-mercaptoethanol) and twice with buffer B (buffer A with 300 mM NaCl instead of 150 mM), and proteins were then eluted by incubation of beads with buffer B containing 250 mM imidazole. The beads were centrifuged at 5000 *g* for 5 min and the supernatant was removed and dialyzed overnight at 4 °C against 30% glycerol (v/v), 50 mM Tris (pH 7.4), 0.15 M NaCl,

and 10 mM β -mercaptoethanol. For *in vitro* arginylation of peptides immobilized on cellulose membranes, reaction samples (90 μ L) consisting of 5.8 μ M [14 C] Arg (PerkinElmer Life Sciences, Waltham, MA, USA, 346 mCi·mmol $^{-1}$), purified total *E. coli* tRNA (0.6 mg·mL $^{-1}$), *E. coli* aminoacyl-tRNA synthetases (800 units·mL $^{-1}$; Merck), 5 mM ATP, 0.15 M KCl, 10 mM MgCl $_2$, 1 mM DTT, and 50 mM Tris-HCl (pH 8.0) were preincubated at 37 °C for 15 min to allow formation of Arg-tRNA. The reaction sample was then mixed with 2 μ g of purified recombinant ATE1 and added to the arrays for 1 h at 37 °C in a humidified chamber. The reaction was stopped by washing the membranes four times with a large excess of Tris-buffered saline-Tween 20 (TBS-T; 1.15 M NaCl, 50 mM Tris-HCl, pH 7.5, 1% Tween 20) and RNase A (10 mg·mL $^{-1}$). The membranes were then washed overnight with TBS-T, air-dried, and exposed for autoradiography. Spot intensities were measured using IMAGEQUANT TL software (GE Healthcare) and normalized using a negative control peptide set. The threshold for identification as an ATE1 arginylated peptide candidate was based on the distribution of intensities. Briefly, the threshold was set to $Q3 + 1.5 \times IQ$, where $Q3$ is the third quartile and IQ the interquartile of the intensity distribution. Peptides present on the CelluSpot[®] array are listed in Table S2.

Statistical analysis

Data were analysed with PRISM software (GraphPad, La Jolla, CA, USA). Values are presented as the means \pm standard error of the mean (SEM) unless noted. Differences between means (from at least three independent assays) were evaluated using Student's *t*-tests for two groups. A *P* value <0.05 was considered significant.

Acknowledgements

We thank Drs Alexander Varshavsky and Brandon Wadas for useful discussions. We thank Gaëlle Legube for her help in the revision process. IL was supported by a Rubenstein Family Postdoctoral fellowship at the Technion and a fellowship from the Fondation ARC at the CBI-MCD. Sanford Burnham Prebys Medical Discovery Institute Shared Resources are supported by an NCI Cancer Center Support Grant (P30 CA030199). IT is supported by FRQS (Fonds de Recherche du Québec-Santé) Senior Award. This work has been supported by the Fondation ARC pour la recherche sur le cancer. The results shown here are in part based upon data generated by the TCGA Research Network: <https://www.cancer.gov/tcga>.

Conflict of interest

ZR is a co-founder of and scientific advisor to Pangea Therapeutics. All other authors declare no competing interests.

Author contributions

IL and ZAR designed the experiments; IL, BF, YF, AIK, EA-H, and PF performed the experiments; IL, BF, HK, TZ, AnK, KB, IT and ZAR analysed the data. IL and ZAR wrote the manuscript.

Data accessibility

The data that support the findings of this study are available in Table S1. These data were derived from the following resources available in the public domain: TCGA SKCM dataset through cBioPortal (<https://www.cbioportal.org>, Skin Cutaneous Melanoma, TCGA PanCancer Atlas, n = 415).

References

- 1 Tasaki T, Sriram SM, Park KS, Kwon YT. The N-end rule pathway. *Annu Rev Biochem*. 2012;**81**:261–89.
- 2 Cha-Molstad H, Sung KS, Hwang J, Kim KA, Yu JE, Yoo YD, et al. Amino-terminal arginylation targets endoplasmic reticulum chaperone BiP for autophagy through p62 binding. *Nat Cell Biol*. 2015;**17**:917–29.
- 3 Zhang F, Patel DM, Colavita K, Rodionova I, Buckley B, Scott DA, et al. Arginylation regulates purine nucleotide biosynthesis by enhancing the activity of phosphoribosyl pyrophosphate synthase. *Nat Commun*. 2015;**6**:1–9.
- 4 Kwon YT. An essential role of N-terminal arginylation in cardiovascular development. *Science*. 2002;**297**:96–9.
- 5 Lian L, Suzuki A, Hayes V, Saha S, Han X, Xu T, et al. Loss of ATE1-mediated arginylation leads to impaired platelet myosin phosphorylation, clot retraction, and in vivo thrombosis formation. *Haematologica*. 2014;**99**:554–60.
- 6 Wang J, Pavlyk I, Vedula P, Sterling S, Leu NA, Dong DW, et al. Arginyltransferase ATE1 is targeted to the neuronal growth cones and regulates neurite outgrowth during brain development. *Dev Biol*. 2017;**430**:41–51.
- 7 Kurosaka S, Leu NA, Zhang F, Bunte R, Saha S, Wang J, et al. Arginylation-dependent neural crest cell migration is essential for mouse development. *PLoS Genet*. 2010;**6**:e1000878.
- 8 Piatkov KI, Brower CS, Varshavsky A. The N-end rule pathway counteracts cell death by destroying proapoptotic protein fragments. *Proc Natl Acad Sci USA*. 2012;**109**:E1839–47.

- 9 Deka K, Saha S. Heat stress induced arginylation of HuR promotes alternative polyadenylation of Hsp70.3 by regulating HuR stability and RNA binding. *Cell Death Differ.* 2020;**28**:730–47.
- 10 Kumar A, Birnbaum MD, Patel DM, Morgan WM, Singh J, Barrientos A, et al. Posttranslational arginylation enzyme Ate1 affects DNA mutagenesis by regulating stress response. *Cell Death Dis.* 2016;**7**:e2378.
- 11 Brower CS, Piatkov KI, Varshavsky A. Neurodegeneration-associated protein fragments as short-lived substrates of the N-end rule pathway. *Mol Cell.* 2013;**50**:161–71.
- 12 Rai R, Zhang F, Colavita K, Leu NA, Kurosaka S, Kumar A, et al. Arginyltransferase suppresses cell tumorigenic potential and inversely correlates with metastases in human cancers. *Oncogene.* 2016;**35**:4058–68.
- 13 Birnbaum MD, Zhao N, Moorthy BT, Patel DM, Kryvenko ON, Heidman L, et al. Reduced Arginyltransferase 1 is a driver and a potential prognostic indicator of prostate cancer metastasis. *Oncogene.* 2018;**386**:838–51.
- 14 Karakozova M, Kozak M, Wong CCL, Bailey AO, Yates JR, Mogilner A, et al. Arginylation of β -actin regulates actin cytoskeleton and cell motility. *Science.* 2006;**313**:192–6.
- 15 Pavlyk I, Leu NA, Vedula P, Kurosaka S, Kashina A. Rapid and dynamic arginylation of the leading edge β -actin is required for cell migration Graphical abstract HHS Public Access. *Traffic.* 2018;**19**:263–72.
- 16 Pavlyk I, Rzhetskiy Y, Jagielski AK, Drozak J, Wasik A, Pereverzieva G, et al. Arginine deprivation affects glioblastoma cell adhesion, invasiveness and actin cytoskeleton organization by impairment of β -actin arginylation. *Amino Acids.* 2015;**47**:199–212.
- 17 Kim HJ, Kim SY, Kim DH, Park JS, Jeong SH, Choi YW, et al. Crosstalk between HSPA5 arginylation and sequential ubiquitination leads to AKT degradation through autophagy flux. *Autophagy.* 2021;**17**:961–79.
- 18 Miller AJ, Mihm MC. Melanoma. *N Engl J Med.* 2006;**355**:51–65.
- 19 Bailey CM, Morrison JA, Kulesa PM. Melanoma revives an embryonic migration program to promote plasticity and invasion. *Pigment Cell Melanoma Res.* 2012;**25**:573–83.
- 20 Kaufman CK, Mosimann C, Fan ZP, Yang S, Thomas AJ, Ablain J, et al. A zebrafish melanoma model reveals emergence of neural crest identity during melanoma initiation. *Science.* 2016;**351**:aad2197.
- 21 Platz A, Egyhazi S, Ringborg U, Hansson J. Human cutaneous melanoma; a review of NRAS and BRAF mutation frequencies in relation to histogenetic subclass and body site. *Mol Oncol.* 2008;**1**:395–405.
- 22 Barretina J, Caponigro G, Stransky N, Venkatesan K, Margolin AA, Kim S, et al. The Cancer Cell Line Encyclopedia enables predictive modelling of anticancer drug sensitivity. *Nature.* 2012;**483**:603–7.
- 23 Jiang C, Moorthy BT, Patel DM, Kumar A, Morgan WM, Alfonso B, et al. Regulation of mitochondrial respiratory chain complex levels, organization, and function by arginyltransferase 1. *Front Cell Dev Biol.* 2020;**8**:603688.
- 24 Zoncu R, Efeyan A, Sabatini DM. mTOR: from growth signal integration to cancer, diabetes and ageing. *Nat Rev Mol Cell Biol.* 2010;**121**:21–35.
- 25 Cargnello M, Roux PP. Activation and function of the MAPKs and their substrates, the MAPK-activated protein kinases. *Microbiol Mol Biol Rev.* 2011;**75**:50–83.
- 26 Wadas B, Piatkov KI, Brower CS, Varshavsky A. Analyzing N-terminal arginylation through the use of peptide arrays and degradation assays. *J Biol Chem.* 2016;**291**:20976–92.
- 27 Zhang Y, Wang X. (2020) Targeting the Wnt/ β -catenin signaling pathway in cancer. *J Hematol Oncol.* 2020;**131**:1–16.
- 28 Xu H, Feng Y, Jia Z, Yang J, Lu X, Li J, et al. AXIN1 protects against testicular germ cell tumors via the PI3K/AKT/mTOR signaling pathway. *Oncol Lett.* 2017;**14**:981.
- 29 Pavey S, Johansson P, Packer L, Taylor J, Stark M, Pollock PM, et al. Microarray expression profiling in melanoma reveals a BRAF mutation signature. *Oncogene.* 2004;**2323**:4060–7.
- 30 Hodis E, Watson IR, Kryukov GV, Arold ST, Imielinski M, Theurillat J-P, et al. A landscape of driver mutations in melanoma. *Cell.* 2012;**150**:251–63.
- 31 Kwong LN, Costello JC, Liu H, Jiang S, Helms TL, Langsdorf AE, et al. Oncogenic NRAS signaling differentially regulates survival and proliferation in melanoma. *Nat Med.* 2012;**1810**:1503–10.
- 32 Kinsey CG, Camolotto SA, Boespflug AM, Guillen KP, Foth M, Truong A, et al. Protective autophagy elicited by RAF→MEK→ERK inhibition suggests a treatment strategy for RAS-driven cancers. *Nat Med.* 2019;**254**:620–7.
- 33 Iranzo J, Martincorena I, Koonin EV. Cancer-mutation network and the number and specificity of driver mutations. *Proc Natl Acad Sci USA.* 2018;**115**:E6010–9.
- 34 Irahara N, Baba Y, Nosho K, Shima K, Yan L, Dias-Santagata D, et al. NRAS mutations are rare in colorectal cancer. *Diagnostic Mol Pathol.* 2010;**19**:157–63.
- 35 Muñoz-Couselo E, Adelantado EZ, Ortiz C, García JS, Garcia JP. NRAS-mutant melanoma: current challenges and future prospect. *Onco Targets Ther.* 2017;**10**:3941–7.
- 36 Tang Z, Kang B, Li C, Chen T, Zhang Z. GEPIA2: an enhanced web server for large-scale expression profiling and interactive analysis. *Nucleic Acids Res.* 2019;**47**:W556–60.

- 37 Leboeuf D, Abakumova T, Prikazchikova T, Rhym L, Anderson DG, Zatsepin TS, et al. Downregulation of the Arg/N-degron pathway sensitizes cancer cells to chemotherapy in vivo. *Mol Ther*. 2020;**28**:1092–104.
- 38 Bronner ME, LeDouarin NM. Development and evolution of the neural crest: an overview. *Dev Biol*. 2012;**366**:2–9.
- 39 Szczyrba J, Niesen A, Wagner M, Wandernoth PM, Aumüller G, Wennemuth G. Neuroendocrine cells of the prostate derive from the neural crest. *J Biol Chem*. 2017;**292**:2021–31.
- 40 MacDonald BT, Tamai K, He X. Wnt/beta-catenin signaling: components, mechanisms, and diseases. *Dev Cell*. 2009;**17**:9–26.
- 41 Taniguchi K, Roberts LR, Aderca IN, Dong X, Qian C, Murphy LM, et al. Mutational spectrum of β -catenin, AXIN1, and AXIN2 in hepatocellular carcinomas and hepatoblastomas. *Oncogene*. 2002;**21**:4863–71.
- 42 Guichard C, Amaddeo G, Imbeaud S, Ladeiro Y, Pelletier L, Maad IB, et al. Integrated analysis of somatic mutations and focal copy-number changes identifies key genes and pathways in hepatocellular carcinoma. *Nat Genet*. 2012;**44**:694–8.
- 43 Li Q, Wang X, Wu X, Rui Y, Liu W, Wang J, et al. Daxx cooperates with the axin/HIPK2/p53 complex to induce cell death. *Cancer Res*. 2007;**67**:66–74.
- 44 Oh J-H, Hyun J-Y, Chen S-J, Varshavsky A. Five enzymes of the Arg/N-degron pathway form a targeting complex: the concept of superchanneling. *Proc Natl Acad Sci USA*. 2020;**117**:10778–88.
- 45 Wingfield PT. N-terminal methionine processing. *Curr Protoc Protein Sci*. 2017;**88**:6.14.1–6.14.3.
- 46 Pa R, Dj M. NH₂-terminal processing of actin in mouse L-cells in vivo. *J Biol Chem*. 1983;**258**:3961–6.
- 47 Wang J, Han X, Saha S, Xu T, Rai R, Zhang F, et al. Arginyltransferase is an ATP-independent self-regulating enzyme that forms distinct functional complexes in vivo. *Chem Biol*. 2011;**18**:121–30.
- 48 Talmadge JE, Fidler IJ. Enhanced metastatic potential of tumor cells harvested from spontaneous metastases of heterogeneous murine tumors. *J Natl Cancer Inst*. 1982;**69**:975–80.
- 49 Lazar I, Fabre B, Feng Y, Khateb A, Turko P, Martinez Gomez JM, et al. SPANX control of lamin A/C modulates nuclear architecture and promotes melanoma growth. *Mol Cancer Res*. 2020;**18**:1560–73.

Supporting information

Additional supporting information may be found online in the Supporting Information section at the end of the article.

Fig. S1. *ATE1* association with melanoma patient age, gender, tumour type and prognosis.

Fig. S2. *ATE1* expression in melanoma cell lines.

Fig. S3. *ATE1* knockdown inhibits melanoma cell migration.

Fig. S4. *ATE1* knockdown inhibits cell viability.

Fig. S5. Inhibition of melanoma cell viability and effect on *ATE1* by serum starvation.

Fig. S6. *ATE1* knockdown modulates activation of mTOR and MAPK signalling pathways.

Fig. S7. AXIN1 level is affected by *ATE1*.

Fig. S8. Higher *ATE1* expression in metastatic NRAS mutant melanomas.

Fig. S9. *ATE1* expression is upregulated in pancreatic cancer samples.

Table S1. List of melanoma patients used in this study.

Table S2. List and sequences of the peptides used for the assay presented in Figure 6.

Data S1. Material & methods.